

RE₂L: An Efficient Output-sensitive Algorithm for Computing Boolean Operation on Circular-arc Polygons

Zhi-Jie Wang, Xiao Lin, Mei-e Fang, Bin Yao, Haibing Guan, and Minyi Guo

Abstract—The boundaries of *conic polygons* consist of conic segments or second degree curves. The conic polygon has two degenerate or special cases: the linear polygon and the circular-arc polygon. The natural problem — boolean operation on linear polygons, has been *well* studied. Surprisingly, (almost) no article *focuses on* the problem of boolean operation on circular-arc polygons, which actually can also find many applications, implying that if there is a targeted solution for boolean operation on circular-arc polygons, which should be favourable for potential users. In this article, we devise a concise data structure, and then develop a targeted algorithm called RE₂L. Our method is surprisingly simple, easy-to-implement but without loss of efficiency. Given two circular-arc polygons with m and n edges respectively, we prove that the proposed method runs in $O(m + n + (l + k) \log l)$ time, using $O(m + n + l + k)$ space, where k is the number of intersections, and l is the number of related edges. The experimental results show our proposed algorithm is significantly faster than the ones that are by directly appealing to the existing algorithms.

Index Terms—Boolean operation, circular-arc polygons, related edges, sequence lists, appendix points

1 INTRODUCTION

Boolean operation on polygons is one of the oldest and best-known problems, and it has attracted much attentions, due to its simple formulation and broad applications in various disciplines such as computational geometry, computer graphics, CAD, GIS, motion planning [6], [7], [8], [11], [17], [26]. When the polygons to be operated are *conic polygons* (whose boundaries consist of conic segments or second degree curves), researchers have made *corresponding* efforts, see, e.g., [5], [9], [1], [2]. The conic polygon has several special or degenerate cases: (i) the linear polygon (known as traditional polygon), whose boundaries consist of only linear curves, i.e., straight line segments; and (ii) the circular-arc polygon, whose boundaries consist of circular-arcs and/or straight line segments. The natural problem — boolean operation on traditional polygons — has been well investigated, see e.g., [24], [20], [10], [16], [14], [21], [19], [17], [12], [3], [13], [15]. Surprisingly, in existing literature, (almost) no article *focuses on* another natural problem — boolean operation on circular-arc polygons. In fact, boolean operation on circular-arc polygons can also find many applications. For instance, deploying sensors to ensure wireless coverage is an important problem [25], [18]. The sensing range of a single sensor is a circle. With obstacles, its sensing range is cut off, shaping a circular-arc polygon. When we verify the wireless coverage range of sensors, boolean operation

on circular-arc polygons is needed. As another example, assume there are a group of free-rotating cameras used to monitor a supermarket. The visual range of a single camera can be regarded as a circle, as it is to be freely rotated. Various obstacles such as goods shelves usually impede the visions of cameras, here boolean operation can be used to check the blind angles. Last but not least, consider a group of free-moving robots used to guide the visitors in a museum. Since the energy of a single robot is limited, its movable region is restricted to a circle. With the impact of various obstacles such as exhibits, the original movable region is to be cut off by these obstacles. When we verify if every place in the museum can be served by at least a robot, boolean operation on circular-arc polygons is also needed.

Although the solution used to handle conic polygons can also work for its special cases, the special cases however, usually have their unique properties; directly appealing to the algorithm used to handle conic polygons is usually not efficient enough. It is just like when the applications only involve traditional polygons, we usually incline to use the solutions targeted for traditional polygons rather than the ones for conic polygons. With the similar argument, when the applications only involve circular-arc polygons, a targeted solution for circular-arc polygons should be favourable for potential users.

Motivated by these, this paper makes the effort to the problem of boolean operation on circular-arc polygons. First of all, a concise and easy-to-operate data structure called APDLL is naturally developed. Based on this concise structure, we propose an algorithm named RE₂L that consists of three main steps. The first step is the kernel of RE₂L, yielding two *special* sequence lists. Specifically, the kernel integrates

- Z.-J. Wang, X. Lin, M.-e Fang, B. Yao, H. Guan, and M. Guo are with the Department of Computer Science and Engineering, Shanghai Jiao Tong University, Shanghai 200240, China. E-mail: zjwang888@sjtu.edu.cn, xiaolin@sjtu.edu.cn, meiefang@cs.sjtu.edu.cn, binyao@cs.sjtu.edu.cn, hbguan@cs.sjtu.edu.cn, guomy@cs.sjtu.edu.cn.

three surprisingly simple yet efficient strategies: (i) it introduces the concept of *related edges*, which is used to avoid irrelevant computation as much as possible; (ii) it employs two *special sequence lists*, each one is a compound structure with three domains; they are used to let the *decomposed arcs*, intersections and *processed related edges* be well organized, and thus immensely simplify the subsequent computation; and (iii) it assigns two *labels* to each processed related edge before the edge is placed into the red-black tree; this contributes to avoiding the “false” intersections being reported, and speeding up the process of inserting the reported intersections into their corresponding edges. The second step of our algorithm produces two *new* linked lists in which the intersections, appendix points, and original vertexes have been arranged, and the decomposed arcs have been merged. To obtain these two new linked lists, two important but easy-to-ignore issues, “inserting new appendix points” and “merging the decomposed arcs”, are addressed. The third step is to obtain the resultant polygon by traversing these two new linked lists. In order to correctly traverse them, the *entry-exit* properties are naturally adopted, and three traversing rules are developed. Given two circular-arc polygons with m and n edges, respectively, we prove that the proposed algorithm runs in $O(m + n + (l + k) * \log l)$ time, using $O(m + n + l + k)$ space. To sum up, we make the following main contributions.

- We highlight the circular-arc polygon is one of special cases of the conic polygon, and boolean operation of circular-arc polygons has also many applications.
- We devise a concise and easy-to-operate data structure, and develop a targeted algorithm for boolean operation on circular-arc polygons.
- We analyse the complexity of our proposed algorithm, and conduct extensive experiments to demonstrate its efficiency and effectiveness.
- While this paper focuses on boolean operation of circular-arc polygons, we show our techniques can be easily extended to compute boolean operation of other types of polygons.

The remainder of the paper is organized as follows. Section 2 reviews previous works most related to ours, and Section 3 introduces the preliminaries, including some basic concepts, the data structure employed by our algorithm, and the top-level framework of our algorithm. Section 4 presents the central ideas of our algorithm. The details of constructing two new linked lists and traversing them are addressed in Section 5 and 6, respectively. Section 7 analyses the time/space complexity of our algorithm. Section 8 evaluates our algorithm based on extensive experiments. Section 9 shows our techniques can be easily extended to compute boolean operation of other types of polygons, and finally Section 10 concludes this paper.

2 RELATED WORK

We first clarify several technical terms for ease of presentation. It is well known that there are three typical boolean operations: intersection, union, and difference. Note that *polygon clipping* mentioned in many papers actually is to compute the *difference* of two polygons [24]. Given two polygons, the one to be clipped is called the *subject polygon*, another is usually called the *clip polygon* or *clip window* [23], [24], [13]. Given a polygon, if there is a pair of non-adjacent edges intersecting with each other, this polygon is usually called the *self-intersection* polygon [3], [10], [21]. Throughout this paper, the *traditional polygon* refers to the polygon whose boundaries consist of *only* straight line segments, *regardless of* whether it is convex or concave. We are now ready to review the previous works most related to ours.

2.1 Boolean operation on traditional polygons

In existing literature, there are many papers studying boolean operation of traditional polygons. For example, Sutherland-Hodgeman [23] proposed an elegant algorithm dealing with the case when the *clip polygon* is convex. Liang et al. [13] gave elaborate analysis on the case when the *clip polygon* is rectangular. Andreev [3] and Greiner-Hormann [10] proposed general algorithms that can handle concave polygons with holes and self-intersections. Later, Liu et al. [14] further optimized Greiner-Hormann’s algorithm. Rivero-Feito [21] achieved boolean operation of polygons based on the concept of *simplicial chains*. Peng et al. [19] also adopted simplicial chains, and improved Rivero-Feito’s algorithm. Recently, Martinez et al. [17] proposed to subdivide the edges at the intersection. These works lay a solid foundation for the future research. Compared to these works, this paper focuses on boolean operation of circular-arc polygons, and thus is different from theirs.

2.2 Boolean operation on conic/general polygons

Researchers have also made corresponding efforts on boolean operation of conic polygons. For example, Berberich et al. [5] proposed to use the *plane sweep method* to achieve boolean operation of conic polygons. Gong et al. [9] achieved boolean operation of conic polygons using the topological relation between two conic polygons, this method does not require *x-monotone* conic arc segments. Both of algorithms can support boolean operation of circular-arc polygons, as the conic polygon is the general case of the circular-arc polygon. Note that the computational geometry algorithms library (CGAL) [1] can also support boolean operation of circular-arc polygons. Inspecting the source codes of CGAL, we realize that its idea is directly appealing to the algorithm of boolean operation on *general polygons*, defined as `GeneralPolygon_2` in

CGAL. To some extent the general polygon can be looked as the most general case, as its edges can be line segments, circular arcs, conic curves, cubic curves, or even more complicated curves. The essence of the algorithm in CGAL is also to use the *plane sweep method*, and is also to use the DCEL structure to represent the (general) polygons, which are similar to that in [5]. These excellent works give us a lot of inspiration, our work yet is different from theirs, as this paper focuses on one of special cases of conic polygon; particularly, we give insights into its unique properties, employ a concise data structure customized for this special case, and develop the targeted algorithm.

3 PRELIMINARIES

3.1 Basic concepts

Definition 1. (Circular-arc polygon) *A polygon is a circular-arc polygon such that its boundaries consist of circular arcs, or both straight line segments and circular arcs.*

Definition 2. (Non-x-monotone circular arc) *Given any circular arc, it is a non-x-monotone circular arc such that there is at least one vertical line that intersects with the circular arc at two points.*

Definition 3. (X-monotone circular arc) *A circular arc is an x-monotone circular arc such that there is at most one intersection with any vertical line.*

Note that in the paper we slightly abuse the term *intersection* but its meaning should be clear from the context.

Theorem 1. (Decompose non-x-monotone circular arc) *Let N_{xmc} be an arbitrary non-x-monotone circular arc, and C be its corresponding circle. Assume that l_h is a horizontal line passing through the center of C . We have that l_h can decompose N_{xmc} into at least two and at most three x-monotone arcs.*

Proof: Since l_h passes through the center of C , it must intersect with C at two points, say p_1 and p_2 . For any non-x-monotone circular arc N_{xmc} , it has only two cases. (i) both p_1 and p_2 are located on N_{xmc} ; and (ii) only p_1 (or p_2) is located on N_{xmc} . For case 1, based on *analytic geometry*, it is easy to know that N_{xmc} will be decomposed into two arcs by l_h when p_1 (or p_2) is the endpoint of N_{xmc} (see Figure 1(a)); otherwise, N_{xmc} will be decomposed into three arcs by l_h (see Figure 1(b)). For case 2, we can also easily know that N_{xmc} will be decomposed into two arcs by l_h (see Figure 1(c)). In addition, both the upper semi-circle and below semi-circle of C are x-monotone arcs; and any sub-arc of upper or below semi-circle is also an x-monotone arc. Pulling all together, hence the theorem holds. \square

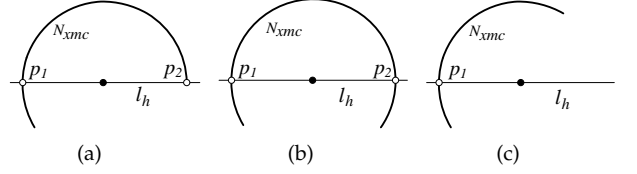


Fig. 1. Illustration of Theorem 1.

3.2 Representation

It is well known that the traditional polygon can be represented by a series of vertices. This method however is invalid for polygons containing circular arcs, as two vertices cannot exactly determine a circular arc segment (note: it may be a major or minor arc). Even so, this ambiguity can be easily eliminated by adding an *appendix point*. For clarity, a traditional vertex is denoted by v_i , and an appendix point is denoted by \tilde{v}_j . For example, $\{v_1, \tilde{v}_2, v_3, v_4, v_5\}$ determine a circular-arc polygon with four edges (including one circular arc segment $\widehat{v_1 \tilde{v}_2 v_3}$ and three straight line segments $\overline{v_3 v_4}$, $\overline{v_4 v_5}$, $\overline{v_5 v_1}$). Unless stated otherwise, in the rest of the paper we always use $\overline{\cdot}$ and $\widehat{\cdot}$ to denote the line segment and the arc segment, respectively. In order to efficiently operate circular-arc polygons, we devise a data structure called APDLL (appendix point based double linked list). Specifically, each node in the double linked list consists of several domains below.

- **Data:** (x, y) , the coordinates of a point.
- **Tag:** Boolean type, it indicates whether this point is a traditional vertex or an appendix point.
- **Crossing:** Boolean type, it indicates whether this point is an intersection.
- **EE:** Boolean type, it indicates what property (*entry* or *exit*) an intersection has.
- **PPointer:** Node pointer, it points to the previous node.
- **NPointer:** Node pointer, it points to the next node.

We remark that the entry-exit property of the intersection is used to traverse, more details about the entry-exit property will be discussed in Section 6. For ease of understanding our proposed method, we next describe the overall framework of our algorithm, and then go into the details.

3.3 Top-level of our algorithm

Let \mathcal{P}_1 and \mathcal{P}_2 respectively denote two circular-arc polygons to be operated, and let \mathcal{P}_3 denote the resultant polygon (i.e., the output of our algorithm). The overall framework of our proposed method is described as follows.

Algorithm 1 RE2L

Input: $\mathcal{P}_1, \mathcal{P}_2$

Output: \mathcal{P}_3

- (1) *ConstructSequenceLists*(\cdot)
 - (2) *ConstructNewLinkedLists*(\cdot)
 - (3) *TraverseLinkedLists*(\cdot)
 - (4) **Return** \mathcal{P}_3
-

The function *ConstructSequenceLists*(\cdot) is used to construct two sequence lists in which the intersections are well organized, and the decomposed arcs are well arranged. Note that this function is the kernel of our algorithm. The function *ConstructNewLinkedLists*(\cdot) is used to construct two new linked lists in which the intersections, appendix points, and original vertexes have been arranged, and the decomposed arcs have been merged. The function *TraverseLinkedLists*(\cdot) is used to obtain the resultant polygon by traversing the two new linked lists.

4 THE KERNEL OF RE2L

4.1 Related edges

One of our strategies is to choose *related edges* before doing others. The purpose of choosing *related edges* is to avoid operations that are irrelevant with obtaining the final result as much as possible. We next show how to obtain the related edges, and inspect their properties.

Definition 4. (Extended boundary lines) *Given a circular-arc polygon, we can always find its minimum bounding rectangle (MBR). Without loss of generality, assume the coordinates of left-bottom corner of the MBR are (x_1, y_1) , the one of right-top corner of the MBR is (x_2, y_2) . Then, the following four lines, $X=x_1$, $X=x_2$, $Y=y_1$, $Y=y_2$ are respectively the left, right, bottom and top extended boundary lines of this circular-arc polygon.*

Definition 5. (Effective axis) *Given two circular-arc polygons \mathcal{P}_1 and \mathcal{P}_2 , let I_{mm} be the intersection set of their MBRs. If the horizontal span of I_{mm} is larger or equal to its vertical span; then, the y-axis is the effective axis. Otherwise, the x-axis is the effective axis.*

Definition 6. (Related edges) *Given two circular-arc polygons \mathcal{P}_1 and \mathcal{P}_2 , we use l_1/l_2 , r_1/r_2 , t_1/t_2 and b_1/b_2 to denote the left, right, top and bottom extended boundary lines of $\mathcal{P}_1/\mathcal{P}_2$, respectively. Without loss of generality, assume the effective axis is the x-axis and $l_1 < l_2 < r_1 < r_2$, where $l_1 < l_2$ denotes l_1 is in the left of l_2 . Then, the following edges are related edges. (i) edges located between l_2 and r_1 ; or (2) edges intersected with l_2 or r_1 .*

See Figure 2(a) for example, edges \overline{ab} and \overline{bc} are *related edges* as they intersect with l_2 . Similarly, edges \overline{de} and \overline{ef} are also *related edges*.

Remark 1. In Definition 6, there are actually other cases, e.g., " $l_1 < l_2 < r_2 < r_1$ " or the effective axis is the y-axis; these cases are similar to the listed case, omitted for saving space.

Definition 7. (Processed related edges) *Given a number of related edges, we decompose them if there are non-x-monotone arcs, we call all the edges (after decomposing) the processed related edges.*

Lemma 1. *Given l related edges, if there is no non-x-monotone arc among them, the number of processed related*

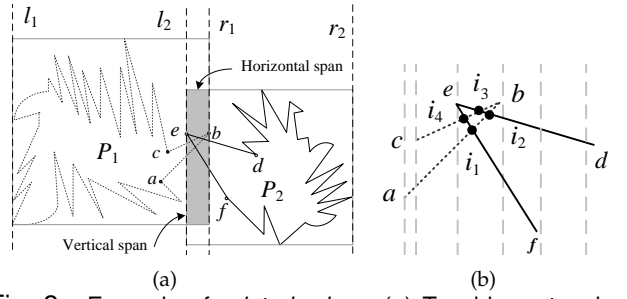


Fig. 2. Example of *related edges*. (a) Two big rectangles denote the MBRs; the grey rectangle denotes the intersection set of two MBRs, and the dashed vertical lines denote the extended boundary lines. (b) Partial enlarged drawing.

edges is l . Otherwise, the number of processed related edges is larger than l and no more than $3l$.

Proof: It is immediate by Theorem 1. \square

Up to now, we have discussed the properties of related edges, and explained how to choose related edges from two circular-arc polygons. We next show how to use two sequence lists to manage the *processed related edges* as well as other important components.

4.2 Two sequence lists

The main purpose of the two sequence lists is to let the processed related edges, intersections and decomposed arcs be well organized, which can facilitate the subsequent operations. Specifically, each item in the two sequence lists is a compound structure consisting of three domains: (i) the processed related edge; (ii) the intersections (if exist) on this edge; and (iii) a trival switch. For ease of discussion, we denote by S_1 and S_2 the two sequence lists, by $S_i[j]$ the j th item in S_i ($i \in 1, 2$), and by $S_i[j].1$, $S_i[j].2$ and $S_i[j].3$ the three domains of $S_i[j]$, respectively.

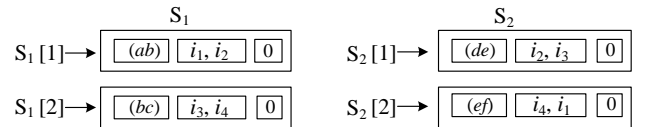


Fig. 3. Example of *sequence lists*.

The processed related edges in each sequence list are stored along the direction of counter-clockwise w.r.t. the original circular-arc polygon. For example, regarding to circular-arc polygons in Figure 2, we construct two sequence lists as shown in Figure 3. Note that when there are multiple intersections on an edge, we should let these intersections in order. See $S_1[1].2$ of Figure 3 for example, the point i_1 is in the front of the point i_2 . Regarding to the third domain $S_i[j].3$, it is assigned to either 0, 1, or 2. The assignment rules are as follows. When the edge is not a decomposed arc, we assign "0" to $S_i[j].3$. In this example, for any $1 \leq j \leq |S_i|$ (where $|\cdot|$ denotes the cardinality of S_i), $S_i[j].3$ is set to 0, as there is no decomposed arc. Otherwise, we assign "1" or "2"

to $S_i[j].3$. The readers may be curious why we use two different values. The purpose is to differentiate the decomposed arcs which are from different non-x-monotone arcs. This can help us efficiently merge them in the future. (The details on how to merge them will be discussed in Section 5.) Given a series of decomposed arcs, we assign “1” to each decomposed arc that is from the 1st (3rd, 5th, ...) non-x-monotone arc, and assign “2” to each decomposed arc that is from the 2nd (4th, 6th, ...) non-x-monotone arc.

See Figure 4(a) for example, there are five *related edges* in \mathcal{P}_1 . Furthermore, Figure 4(b) illustrates eight *processed related edges* (after we decompose them based on Theorem 1), implying that $|S_1| = 8$. Based on the assignment rules, the values of the third domains should be “0, 1, 1, 2, 2, 1, 1, 0”, respectively.

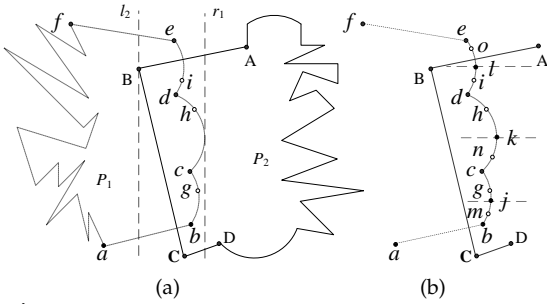


Fig. 4. Example of consecutive non-x-monotone circular arcs. (a) Edges $\widehat{ab}, \widehat{bgc}, \widehat{chd}, \widehat{die}, \widehat{eaf}$ are *related edges* of \mathcal{P}_1 . (b) Edges $\widehat{ab}, \widehat{bmj}, \widehat{jgc}, \widehat{cnk}, \widehat{khd}, \widehat{dil}, \widehat{loe}, \widehat{eaf}$ are *processed related edges* of \mathcal{P}_1 ; three dashed lines are the auxiliary lines.

Thus far, we have shown how to use two sequence lists to manage the processed related edges and intersections. Note that, in order to obtain the intersections, a standard method is the *plane sweep method* algorithm [4], [22]. In this paper, we do not directly use this algorithm. Instead, we add *two labels* to avoid the “false” intersections being reported, and to speed up the process of inserting the reported intersections into their corresponding edges. (Remark: here the *false* intersections refer to the vertexes of polygons.) We next give a brief review of the plane sweep algorithm, and then show more details about the two labels.

Plane sweep method. Let \mathcal{Q} be a heap, \mathcal{R} be a red black tree, and l_v be a vertical sweep line. The basic idea of the plane sweep method is as follows. First, it sorts the endpoints of all segments according to their x-coordinates, and then puts them into \mathcal{Q} . Next, it sweeps the plane (from left to right) using l_v . At each endpoint during this sweep, if an endpoint is the left endpoint of a segment, it inserts this segment into \mathcal{R} ; in contrast, if it is the right endpoint of a segment, it deletes this segment from \mathcal{R} . Note that all the segments intersecting with l_v are stored (in order from bottom to top) in \mathcal{R} . In particular, when l_v moves from one endpoint to another endpoint, it always checks whether or not newly adjacent segments intersect

with each other; If so, it computes the intersection. In this way, all intersections can be obtained finally.

4.3 Two labels

We can easily see that the plane sweep method directly inserts a segment into the red-black tree \mathcal{R} , if the point p ($\in \mathcal{Q}$) is the left endpoint of the segment. Instead, we assign two labels to the segment before it is inserted into \mathcal{R} . Note that the segment discussed here refers to the *processed related edge*. For clearness, we denote by lb_1 and lb_2 the two labels, respectively.

lb_1 is the boolean type, identifying that a segment is from which one of the two circular-arc polygons. Specifically, if the segment is from \mathcal{P}_1 , we assign *true* to lb_1 ; otherwise, we assign *false* to lb_1 . Recall that the plane sweep method always checks whether or not two segments intersect with each other, when they are adjacent. Our proposed method do not need to check them regardless of whether or not they intersect, if the first labels of two adjacent edges have the same value. This can avoid the unnecessary test and the “false” intersections.

lb_2 is an integer type denoting a serial number, which corresponds to the “id” of an item stored in the sequence list (note: the “id” information of each item is implied, as we adopt the sequence list to store the items). When we detected an intersection, this label can help us quickly find the item in the sequence list, and then insert the intersection into this item. See Figure 2(b) for example, lb_1 and lb_2 of edge \widehat{ab} are assigned to *true* and 1, respectively. When we detected the intersection i_1 , we thus can quickly know that we should insert the intersection into $S_1[1]$ (i.e., the first item of S_1). Otherwise, we have to scan the sequence list in order to insert the intersection into an appropriate item, this way is inefficient especially when $|S_1|$ (or $|S_2|$) is large.

4.4 The algorithm

Let R_1 and R_2 be the related edges from \mathcal{P}_1 and \mathcal{P}_2 , respectively. Given a segment s , we use $s.lb_1$ and $s.lb_2$ to denote the two labels of segment s . Algorithm 2 below illustrates the pseudo-codes of constructing the two sequence lists.

Algorithm 2 ConstructSequenceLists

Input: $\mathcal{P}_1, \mathcal{P}_2$

Output: S_1 and S_2, R_1 and R_2

- (1) Find the MBRs, effective axis and extended boundary lines
- (2) $R_i \leftarrow$ related edges from \mathcal{P}_i // where $i \in \{1, 2\}$
- (3) Create two empty sequence lists S_1 and S_2
- (4) **for** each $i \in \{1, 2\}$
- (5) InitializeSequenceList (\cdot) // cf. Algorithm 3
- (6) Sort the endpoints of the segments (from S_1, S_2), and put them into \mathcal{Q}
- (7) $\mathcal{R} \leftarrow \emptyset$ // \mathcal{R} is a red-black tree
- (8) **for** each point $p \in \mathcal{Q}$
- (9) Let s be the segment containing the point p , and t be the segment immediately above or below s
- (10) **if** (p is the left endpoint of segment s)
- (11) Assign two “labels” to s , and insert s into \mathcal{R}

```

(12)   if (  $s.lb_1 \neq t.lb_1$  )
(13)       if (  $s$  intersects with  $t$  )
(14)           Insert the intersection into  $\mathcal{Q}$ , and also insert it
              into  $S_1$  and  $S_2$ , respectively
(15)   else if (  $p$  is the right endpoint of segment  $s$  )
(16)       if (  $s.lb_1 \neq t.lb_1$  )
(17)           if (  $s$  intersects with  $t$  and this intersection  $\notin \mathcal{Q}$  )
(18)               Insert this intersection into  $\mathcal{Q}$ , and also insert it
                  into  $S_1$  and  $S_2$ , respectively; delete  $s$  from  $\mathcal{R}$ 
(19)   else //  $p$  is an intersection of two segments, say  $s$  and  $t$ 
(20)       Swap the position of  $s$  and  $t$  // assume  $s$  is above  $t$ 
(20)       Let  $t_1$  be the segment above  $s$ , and  $t_2$  be
              the segment below  $t$ 
(21)       if (  $s.lb_1 \neq t_1.lb_1$  or  $t.lb_1 \neq t_2.lb_1$  )
(22)           if (  $s$  intersects with  $t_1$ , or  $t$  intersects with  $t_2$  )
(23)               Insert the intersection point into  $\mathcal{Q}$ , and also insert
                  it into  $S_1$  and  $S_2$ , respectively
(24)   return  $S_1$  and  $S_2$ ,  $R_1$  and  $R_2$ 

```

We first choose the *related edges* based on the extended boundary lines (Lines 1-2). Next, we construct two empty sequence lists and initialize them (Lines 3-5). After this, we compute the intersections (Lines 6-23). In particular, when we compute the intersections, two *labels* are assigned to the segment before it is inserted into the red-black tree (Line 11), and we use the two sequence lists to store the intersections (Lines 14, 18 and 23). Note that, the pseudo-codes of initializing the two sequence lists are depicted in Algorithm 3. This algorithm decomposes non-x-monotone arcs, puts the *processed related edges* into the sequence lists in an orderly manner, and assigns appropriate values to the tri-value switches.

Algorithm 3 *InitializeSequenceList*

Input: R_i, S_i

Output: S_i

```

(1)  $temp \leftarrow 1$  // the  $temp$  is used to set the tri-value switch
(2) for each related edge  $r \in R_i$ 
(3)   if (  $r$  is a non-x-monotone circular arc )
(4)       Decompose it and put the decomposed arcs into  $S_i$ ,
           and set the value of each tri-value switch to " $temp$ "
(5)   if (  $temp=1$  )
(6)        $temp \leftarrow 2$ ;
(7)   else //  $temp=2$ 
(8)        $temp \leftarrow 1$ ;
(9)   else //  $r$  is not a non-x-monotone circular arc
(10)      Put it into  $S_i$ , set the value of tri-value switch to "0"

```

Theorem 2. *Given two circular-arc polygons with m and n edges, respectively, and assume there are l related edges between the two polygons, we have that constructing the two sequence lists can be finished in $O(m + n + l + (l + k) \log l)$ time, where k is the number of intersections.*

Proof: To obtain the *related edges*, we first need to find the MBRs of two polygons, which takes linear time. We next determine the *effective axis* by comparing the horizontal and vertical spans of the intersection set of two MBRs, which can be finished in constant time. Furthermore, the *extended boundary lines* can be obtained in constant time once we obtain the *effective axis*. Based on two extended boundary lines, we finally obtain the *related edges* by comparing the geometrical relationship between each edge and extended boundary lines, which also takes linear time. Thus, Lines 1-2 take $O(m + n)$ time.

Creating two empty sequence lists takes constant time. In addition, in order to initialize the two sequence lists, we need to decompose each non-x-monotone arc. Decomposing a single arc can be finished in constant time. In the worst case, all the *related edges* are non-x-monotone arcs. Even so, there are no more than $3l$ items in the two sequence lists, according to Theorem 1. So, initializing two sequence lists takes $O(l)$ time. Sorting all the endpoints of segments in the heap \mathcal{Q} takes $O(l \log l)$ time, and initializing the red-black tree \mathcal{R} takes constant time. Thus, Lines 3-7 take $O(l + l \log l)$ time.

As there are no more than $3l$ segments in S_1 and S_2 , the number of endpoints thus is no more than $6l$. So we can easily know that the number of executions of the **for** loop (Line 8) is no more than $6l + k$. Within the **for** loop, each operation (e.g., insert, delete, swap, find the above/below segment) on \mathcal{R} can be finished in $O(\log l)$ time, as the number of segments in \mathcal{R} never exceeds $3l$. Additionally, each of other operations (e.g., assign labels to the segment, determine if two segments intersects with each other) can be finished in constant time. Thus, Lines 8-23 takes $O((6l + k) \log l)$ time, i.e., $O((l + k) \log l)$ time. At last returning the results takes constant time (Line 24). Pulling all together, hence the theorem holds. \square

We have shown how to construct two sequence lists used to manage the *processed related edges* and intersections. Based on the two sequence lists, we next explain how to construct two *new* linked lists used to obtain the resultant polygon.

Remark 2. Recall Section 3.2, the input polygons \mathcal{P}_1 and \mathcal{P}_2 are also stored using linked lists. Unless stated otherwise, the terms "input polygons" and "original linked lists" are used interchangeably in the rest of the paper.

5 TWO NEW LINKED LISTS

It is pretty simple to construct two new linked lists, based on the two sequence lists obtained in the previous step. By the large, we use the information stored in two sequence lists to replace those *related edges* in original linked lists. Note that there are two important yet easy-to-ignore issues needed to be handled when we construct new linked lists. We next check more details about these issues, and then present the algorithm of constructing new linked lists.

5.1 New appendix points

Recall Section 3.2, we always add an *appendix point* between two vertexes if an edge is a circular arc. When we replace *related edges* with the information stored in sequence lists, we also have to ensure this property. It is easy to know that, when the intersections appear on a circular arc, this arc will be decomposed by these intersections. We thus have to add the new appendix point for each sub-segment, in order to eliminate the ambiguity.

Theorem 3. Suppose there are k intersections on a circular arc; then, we need to insert at least k and at most $k + 1$ new appendix points.

Proof: Since k intersections can subdivide a complete circular arc into $k + 1$ small circular arcs, and for each small circular arc one *appendix point* is needed and enough to eliminate the ambiguity. Clearly, $k + 1$ *appendix points* are needed for $k + 1$ small circular arcs. Furthermore, there is an *appendix point* beforehand. Therefore, when there is no intersection coinciding with this *appendix point*, only k new *appendix points* are needed. Otherwise, we need $k + 1$ new *appendix points*. \square

Besides the above issue, another issue is to handle the decomposed arcs. We decomposed non-x-monotone arcs into x-monotone arcs ever, we thus need to merge them. The natural solution is to compare each pair of adjacent edges of the resultant polygon, checking if they can be merged into a single arc. This way however is inefficient because (i) most of edges of the resultant polygon may not need to be merged; and (ii) given two adjacent arcs, let C_1 and C_2 respectively denote their corresponding circles; checking if the two arcs can be merged into a single arc needs to compute the centres of C_1 and C_2 , this will use trigonometric functions (which could have been avoided). We next show how to efficiently merge them, in the aid of the sequence lists.

5.2 Decomposed arcs

We merge the decomposed arcs when constructing new linked lists, rather than merge them after obtaining the resultant polygon. In particular, we here utilize the information stored in the tri-value switch to improve the efficiency. Specifically, given an item $S_i[j]$, if $S_i[j].3 = 1$ (or 2), we continue to fetch its next item $S_i[j + 1]$ from the sequence list if $S_i[j].3 = S_i[j + 1].3$. In this way, a group of consecutive items are fetched from the sequence list. Without loss of generality, assume that we have fetched ϵ consecutive items, $S_i[j], \dots, S_i[j + \epsilon - 1]$. Then, we do as follows.

- If $S_i[j].2 = S_i[j + 1].2 = \dots = S_i[j + \epsilon - 1].2 = \emptyset$, we discard the fetched items instead of merging them. This is because there is no intersection on these decomposed arcs, the merged result should be the same as the edge in the original linked list.
- Otherwise, we insert new appendix points, merge decomposed arcs, and replace the edge in the original linked list.

Let us revisit Figure 4(b); recall that there are eight items in S_1 , and the values in their tri-value switches are “0, 1, 1, 2, 2, 1, 1, 0”, respectively. Although $S_1[2].3 = S_1[3].3 = 1$, we discard the two items instead of merging them, as $S_1[2].2 = S_1[3].2 = \emptyset$. Similarly, we also discard the items $S_1[4]$ and $S_1[5]$. Note that, for the 6th and 7th items, $S_1[6].3 = S_1[7].3 = 1$ and

$S_1[7].2 \neq \emptyset$; thus, we insert a new appendix point, merge the two decomposed arcs, and use the merged result to replace the edge in the original linked list.

Note that, the consecutive items mentioned earlier are actually the decomposed arcs generated from a single non-x-monotone circular arc. According to Theorem 1, we can easily build the following theorem.

Theorem 4. Let ϵ be the number of consecutive items, we have that $\epsilon \leq 3$ and $\epsilon \geq 2$.

5.3 The algorithm

Let \mathcal{P}_1^* and \mathcal{P}_2^* be the two new linked lists, respectively. Algorithm 4 below depicts the pseudo-codes of constructing two new linked lists. For each edge e in the *original linked list*, we check whether it is a *related edge*. If so, we further check whether $S_i[j]$ is a decomposed arc. Lines 7-13 are used to deal with the case when it is not a decomposed arc. In contrast, Lines 14-22 are used to handle the opposite case. In this case, we first fetch all the consecutive decomposed arcs (Lines 15-18), and then check if there are intersections on these decomposed arcs. If it is not, we put the edge e into \mathcal{P}_i^* (Lines 19-20). Otherwise, we insert new appendix points, merge decomposed arcs, and put the merged result (instead of e) into \mathcal{P}_i^* (Lines 21-22).

Algorithm 4 ConstructNewLinkedLists

Input: \mathcal{P}_1 and \mathcal{P}_2 , S_1 and S_2 , R_1 and R_2

Output: \mathcal{P}_1^* and \mathcal{P}_2^*

```

(1) Set  $\mathcal{P}_1^* = \mathcal{P}_2^* = \emptyset$ , and  $j \leftarrow 1$ 
(2) for each  $i \in \{1, 2\}$ 
(3)   for each edge  $e \in \mathcal{P}_i$ 
(4)     if ( $e \notin R_i$ )
(5)       Add  $e$  to  $\mathcal{P}_i^*$ 
(6)     else //  $e$  is a related edge
(7)       if ( $S_i[j].3 = 0$ ) // not a decomposed arc
(8)         if ( $S_i[j].2 = \emptyset$ ) // no intersection
(9)            $j \leftarrow j + 1$ , and add  $e$  to  $\mathcal{P}_i^*$ 
(10)        else //  $S_i[j].2 \neq \emptyset$ 
(11)          if ( $S_i[j]$  is a circular arc)
(12)            Insert new appendix points
(13)            Put the information from  $S_i[j]$  into  $\mathcal{P}_i^*$ , and
              set  $j \leftarrow j + 1$ 
(14)        else //  $S_i[j].3 = 1$  (or 2)
(15)          Set  $tri = S_i[j].3$ , and  $\epsilon \leftarrow 0$ 
(16)          do // copy the consecutive decomposed arcs
(17)             $\epsilon \leftarrow \epsilon + 1$ ,  $temp[c] \leftarrow S_i[j]$ ,  $j \leftarrow j + 1$ 
(18)          while  $S_i[j].3 = tri$ 
(19)          if ( $temp[1].2 = \dots = temp[\epsilon].2 = \emptyset$ )
(20)            Put  $e$  into  $\mathcal{P}_i^*$ 
(21)          else
(22)            Insert new appendix points, merge decomposed
              arcs, and put the merged result into  $\mathcal{P}_i^*$ 
(23) return  $\mathcal{P}_1^*$  and  $\mathcal{P}_2^*$ 
```

Theorem 5. Suppose we have obtained the two sequence lists S_1 and S_2 ; then, constructing the two new linked lists \mathcal{P}_1^* and \mathcal{P}_2^* takes $O(m + n + l + k)$ time.

Proof: Inserting a single *appendix point* takes constant time. In the worst case, all the intersections are located on arcs rather than on line segments. Even so, there are no more than $2k$ new *appendix points* according to Theorem 3. Thus inserting *appendix points* takes $O(k)$ time. Merging ϵ consecutive decomposed

arcs takes constant time, as $\epsilon \leq 3$. In the worst case, all the related edges are non-x-monotone arcs, hence merging all consecutive decomposed arcs takes $O(l)$ time.

Since the number of edges in \mathcal{P}_1 and \mathcal{P}_2 is $m + n$, the number of executions of the second **for** loop (Line 3) is $m + n$. Specifically, the number of executions of Line 4 is $m + n - l$, and the one of Line 6 is l . Even if all related edges are non-x-monotone arcs, the number of executions of Line 17 is no more than $3l$. Furthermore, within the **for** loop, each operation takes constant time (note: here we no longer consider the time for inserting new appendix points and merging decomposed arcs, as we have analysed them in the previous paragraph). Therefore, Lines 4-5 and Lines 7-22 take $O(m + n - l)$ and $O(3l)$ time, respectively. Pulling all together, this completes the proof. \square

To this step, we have obtained \mathcal{P}_1^* and \mathcal{P}_2^* . We next show how to traverse them in order to obtain the resultant polygon.

6 TRAVERSING

In order to correctly traverse the two linked lists, we need to assign the *entry-exit* properties to intersections.

6.1 Entry-exit property

The entry-exit property is an important symbol that was ever used in many papers focusing on boolean operation of traditional polygons (see e.g., [10], [14]). This technique can be equivalently used to the case of our concern. It is quite straightforward to assign the intersections with such properties. Specifically, we assign the intersections with the *entry* or *exit* property *alternately*.

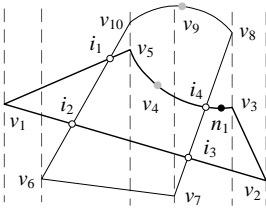


Fig. 5. Two simple circular-arc polygons. $\mathcal{P}_1 = \{v_1, v_2, v_3, \tilde{v}_4, v_5\}$ and $\mathcal{P}_2 = \{v_6, v_7, v_8, \tilde{v}_9, v_{10}\}$.

See Figure 5 for example. \mathcal{P}_1 and \mathcal{P}_2 are two input polygons. We can easily obtain the two new linked lists \mathcal{P}_1^* and \mathcal{P}_2^* using algorithms discussed before. Here $\mathcal{P}_1^* = \{v_1, i_2, i_3, v_2, v_3, \tilde{n}_1, i_4, \tilde{v}_4, v_5, i_1\}$, and $\mathcal{P}_2^* = \{v_6, v_7, i_3, i_4, v_8, \tilde{v}_9, v_{10}, i_1, i_2\}$. Regarding to \mathcal{P}_1^* , we assign “*entry, exit, entry, exit*” to “ i_2, i_3, i_4, i_1 ”, respectively. The *entry-exit* properties of “ i_2, i_3, i_4, i_1 ” in \mathcal{P}_2^* are the same as the ones in \mathcal{P}_1^* . See Figure 6(a).

Once the *entry-exit* properties are assigned to intersections, we then obtain the resultant polygon based on the traversing rules below.

6.2 Traversing rules

Let i_s be an intersection point of \mathcal{P}_1^* such that i_s has the *entry* property. Let v_s be a vertex of \mathcal{P}_1^* such that v_s does not locate in \mathcal{P}_2^* . There are three typical boolean operations: intersection, union and difference. We next discuss their traversing rules, respectively. Note that in the rest of discussion, the default traversing direction is counter-clockwise, unless stated otherwise.

6.2.1 Intersection

We start to traverse \mathcal{P}_1^* using i_s as the starting point. Once we meet an intersection point with the *exit* property, we shift to \mathcal{P}_2^* , and traverse it. Similarly, if we meet an intersection point with the *entry* property in \mathcal{P}_2^* , we shift back to \mathcal{P}_1^* . In this way, a circuit will be produced. After this, we check if there is another intersection point of \mathcal{P}_1^* such that (i) it has the *entry* property; and (ii) it is not a vertex of the produced circuit. If no such an intersection point, we terminate the traversal, and this circuit is the intersection between \mathcal{P}_1 and \mathcal{P}_2 . Otherwise, we let this intersection point as a new starting point, and traverse the two new linked lists (using the same method discussed just now), until no such an intersection point exists. In the end, we get multiple circuits, which are the intersection between \mathcal{P}_1 and \mathcal{P}_2 . See Figure 6(b) for example, we first choose i_2 in \mathcal{P}_1^* as the starting point, and then traverse the two linked lists, getting a circuit (see the dashed lines). Moreover, there is no other intersection point satisfying the two conditions mentioned before. Therefore, the intersection is $\{i_2, i_3, i_4, \tilde{v}_4, v_5, i_1\}$.

6.2.2 Union

We start to traverse \mathcal{P}_1^* using v_s as the starting point. Once we meet an intersection point with the *entry* property, we shift to \mathcal{P}_2^* , and traverse it. Similarly, if we meet an intersection point with the *exit* property in \mathcal{P}_2^* , we shift back to \mathcal{P}_1^* . In this way, a circuit will be produced, which is the union between \mathcal{P}_1 and \mathcal{P}_2 . See Figure 6(c) for example, we first choose v_1 as the starting point, and then traverse the two linked lists, until we are back to the starting point v_1 . Therefore, $\{v_1, i_2, v_6, v_7, i_3, v_2, v_3, \tilde{n}_1, i_4, v_8, \tilde{v}_9, v_{10}, i_1\}$ is the union between \mathcal{P}_1 and \mathcal{P}_2 .

6.2.3 Difference

We start to traverse \mathcal{P}_1^* using v_s as the starting point. Once we meet an intersection point with the *entry* property, we shift to \mathcal{P}_2^* , but traverse along the direction of clockwise. Similarly, if we meet an intersection point with the *exit* property in \mathcal{P}_2^* , we shift back to \mathcal{P}_1^* . In this way, a circuit will be produced. Furthermore, we check if there is another vertex of \mathcal{P}_1^* such that (i) it is not a vertex of any produced circuit; and (ii) it does not locate in \mathcal{P}_2^* . If no such a vertex, we terminate the traversal, and this circuit is the difference between \mathcal{P}_1 and \mathcal{P}_2 . Otherwise, we let the vertex as a new

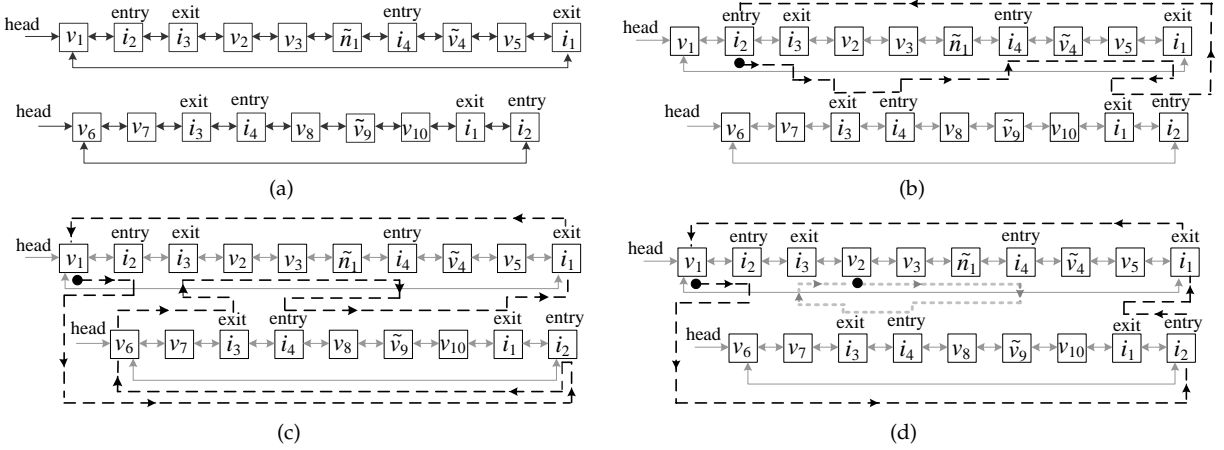


Fig. 6. Illustrations of entry-exit properties and traversing rules. (a) Entry-exit properties of \mathcal{P}_1^* and \mathcal{P}_2^* . (b) Intersection operation. (c) Union operation. (d) Difference operation.

starting point, and traverse the two new linked lists (using the same method discussed just now), until no such a vertex exists. In the end, we get multiple circuits, which are the difference between \mathcal{P}_1 and \mathcal{P}_2 . See Figure 6(d) for example, we first choose v_1 as the starting point, and begin to traverse. Since i_2 has the *entry* property, we shift to \mathcal{P}_2^* (note: we traverse \mathcal{P}_2^* along the direction of clockwise, the next node of i_2 thus is i_1). Since i_1 has the *exit* property, we shift back to \mathcal{P}_1^* . In this way, we get a circuit (see the black dashed lines). After this, we choose v_2 as a new starting point since it satisfies the two conditions mentioned above, and then continue to traverse, getting another circuit (see the grey dashed lines). Thus, the difference between \mathcal{P}_1 and \mathcal{P}_2 consists of two parts, i.e., $\{v_1, i_2, i_1\}$ and $\{v_2, v_3, \tilde{n}_1, i_4, i_3\}$.

6.3 The algorithm

In some cases the result consists of multiple circuits, we denote by l_j the linked list used to store the j th circuit. Let n_d be a node of \mathcal{P}_i^* where $i \in \{1, 2\}$, we denote by c_n the current node when we traverse \mathcal{P}_i^* , and denote by $c_n.next$ the next node of c_n . Furthermore, we denote by i'_s the intersection point of \mathcal{P}_1^* such that i'_s has the entry property and it is not an vertex of any produced circuit, and we use $\exists(i'_s) = true$ to denote there exists such a point. Algorithm 5 below illustrates the pseudo-codes used to obtain the intersection result. (Remark: the pseudo-codes of other two operations can be easily constructed based on the traversing rules, and are the similar as this algorithm, we here omit them for saving space.)

Algorithm 5 *TraverseLinkedLists*

Input: \mathcal{P}_1^* and \mathcal{P}_2^*
Output: \mathcal{P}_3

- (1) Set $j = 1$
- (2) **for** each $i \in \{1, 2\}$
- (3) Assign entry-exit property to \mathcal{P}_i^*
- (4) **do**
- (5) **if** ($j=1$)
- (6) Choose a starting point i_s from \mathcal{P}_1^*

- (7) **else**
- (8) Let $i_s \leftarrow i'_s$ // i.e., let i'_s be a new starting point
- (9) Set $c_n \leftarrow i_s$, and $l_j = \emptyset$
- (10) **do**
- (11) Put c_n into l_j
- (12) **if** ($c_n.next$ is not an intersection point)
- (13) Let $c_n \leftarrow c_n.next$, and put c_n into l_j
- (14) **else**
- (15) Shift to \mathcal{P}_2^* , choose the node n_d such that
- (16) $n_d = c_n.next$, let $c_n \leftarrow n_d$, and put c_n into l_j
- (17) **if** ($c_n.next$ is not an intersection point)
- (18) $c_n \leftarrow c_n.next$, and put c_n into l_j
- (19) **else**
- (20) Shift to \mathcal{P}_1^* , choose the node n_d such that
- (21) $n_d = c_n.next$, and let $c_n \leftarrow n_d$
- (22) **while** ($c_n \neq i_s$)
- (23) Let $\mathcal{P}_3 \leftarrow \mathcal{P}_3 \cup l_j$, and set $j \leftarrow j + 1$
- (24) **while** ($\exists(i'_s) = true$)
- (25) **return** \mathcal{P}_3

Theorem 6. Given the two new linked lists \mathcal{P}_1^* and \mathcal{P}_2^* , to obtain the resultant polygon takes $O(k + m + n + l)$ time.

Proof: Assigning the *entry-exit* property to each intersection takes constant time, and there are k intersections on each new linked list. Thus, assigning *entry-exit* properties to intersections takes $O(k)$ time.

\mathcal{P}_1^* and \mathcal{P}_2^* are used to generate the resultant polygon, they store the vertexes, *appendix* points, and intersections. The number of vertexes is $2(m + n)$. In the worst case, all edges of two input polygons are circular arc segments, implying that the number of *appendix* points in the input polygons is $m + n$; in this case, all the k intersections are located on arcs, we need to insert new *appendix* points, and the number of new *appendix* points is no more than $k + 1$, according to Theorem 3. So the number of all *appendix* points in \mathcal{P}_1^* and \mathcal{P}_2^* is no more than $m + n + k + 1$. Therefore, the total number of nodes in \mathcal{P}_1^* and \mathcal{P}_2^* is no more than $3(m + n) + 2k + 1$. Further, each operation on a node (e.g., determine the type of a node, insert a node into the resultant polygon) takes constant time. Therefore, the traversal takes $O(3(m + n) + 2k + 1)$ time. Pulling the above results together, we have that obtaining the resultant polygon takes $O(m + n + k + l)$ time when \mathcal{P}_1^* and \mathcal{P}_2^* are given beforehand. \square

Up to now, we have addressed all the main steps of our algorithm — RE2L. We next analyse its complexity.

7 TIME/SPACE COMPLEXITY

We analyse the complexity of our algorithm *using* the intersection operation as a sample (note: the complexity of other two operations is the same as the one of this operation, and can be derived similarly, omitted for saving space).

Theorem 7. *Given two circular-arc polygons with m and n edges, respectively, and assume there are l related edges between the two circular-arc polygons. Then, to achieve boolean operation on them takes $O(m + n + (l + k) \log l)$ time, using $O(m + n + l + k)$ space, where k is the number of intersections.*

Proof: Our algorithm consists three main steps, and they take time $O(m + n + l + (l + k) \log l)$, $O(m + n + k + l)$, and $O(m + n + k + l)$, respectively (see Theorem 2, 5 and 6). Pulling these results together, thus the time complexity is $O(m + n + (l + k) \log l)$.

The space used in our algorithm mainly consists of two linked lists \mathcal{P}_1 and \mathcal{P}_2 , two group of related edges R_1 and R_2 , two sequence lists S_1 and S_2 , the heap \mathcal{Q} , two new linked lists \mathcal{P}_1^* and \mathcal{P}_2^* , and the resultant polygon \mathcal{P}_3 (remark: others are minor compared to the space used by these entities. For example, the red-black tree \mathcal{R} stores the segments *currently* intersecting with the sweep line, it has only the constant descriptive complexity). Note that, \mathcal{P}_1 , \mathcal{P}_2 , and \mathcal{P}_3 are used to store the input and output data. By the convention, we do not consider them when we analysis the space complexity. Thus the auxiliary space used by the algorithm mainly consists of R_1 , R_2 , S_1 , S_2 , \mathcal{Q} , \mathcal{P}_1^* and \mathcal{P}_2^* .

Specifically, R_1 and R_2 have the size of $O(l)$, as they are used to store the *related edges*. S_1 and S_2 are used to store the *processed related edges*. In the worst case, the number of *processed related edges* is no more than $3l$, according to Lemma 1. So S_1 and S_2 have the size of $O(3l)$. Recall Algorithm 2, the heap \mathcal{Q} is used to store the endpoints of *processed related edges* and the intersections. So \mathcal{Q} has the size of $O(6l + k)$. Furthermore, \mathcal{P}_1^* and \mathcal{P}_2^* have the size of $O(3(m + n) + 2k + 1)$, see the proof of Theorem 6. Pulling all together, the space complexity of our algorithm is $O(m + n + k + l)$. \square

8 PERFORMANCE EVALUATION

8.1 Methodologies

To investigate the efficiency and effective, we compare our method (i.e., RE2L) with several baseline methods, which are either the algorithms used to handle more general case of polygons, or the simpler versions of our proposed method. We next shortly introduce these methods.

Berberich. We directly appeal to the algorithm in [5], which is initially developed for computing boolean operations of conic polygons. This method employs the DCEL structure to represent the polygons. It first decomposes non-x-monotone conic curves (of two polygons) and then computes the arrangement of segments using the plane sweep method; next, it uses the results of arrangement to compute the *overlap* of two polygons in order to achieve boolean operation. Our implementation also uses the components of LEAD and CGAL by following the guidance of [5]. (Note: more information about the DCEL structure and computing the overlap of two polygons please refer to Chapter 2 of [6].)

CGAL. We directly use the implementation of CGAL. Its essence is to directly appeal to the algorithm of boolean operation on *general polygons*, defined as `GeneralPolygon_2` in CGAL; this algorithm is (almost) the same as the one in [5], recall Section 2.

Naïve. It is one of simpler versions of our proposed method. This method employs our proposed data structure, it however computes the intersections by comparing each pair of edges. Specifically, for each edge of \mathcal{P}_1 , it checks whether it intersects with the edges of \mathcal{P}_2 . If so, it computes the intersections. After all edges of \mathcal{P}_1 are processed, the rest of steps are to assign the *entry-exit* properties and to traverse, which are the same as the ones of our proposed method.

Standard. It is also a simpler version of our proposed method, but it is different from the previous one. Specifically, it employs the standard sweep-line algorithm to compute the intersections instead of checking each pair of edges. Note that it does not adopt the optimization strategies proposed in this paper, others are the same as the previous one.

8.2 Experimental settings

All the algorithms are implemented in C++ language, the experiments are conducted on a computer with 2.16GHz dual core CPU and 1.86GB of memory. In the first set of experiments, we manually produce two circular-arc polygons with less edges for simplicity and for ease of reproducing the findings. The vertex coordinates of the two polygons are listed in Table 1. We run 100 times for each algorithm using the two polygons as the input, and then compute the average running time.

Polygon	Coordinates
\mathcal{P}_1	(10,10), (40,10), (40,30), (32.5,40), (20,40), (15,30), (25,22.5), (15,15)
\mathcal{P}_2	(20,20), (32.5,25), (45,20), (55,30), (35,35.625), (50,50), (30,45)

TABLE 1

The coordinates of vertexes are listed counter-clockwise, and the left-bottom vertex is listed at first. The values tagged with “_” denote the coordinates of *appendix points*.

In the second set of experiments, we adopt thousands of circular-arc polygons, in order to study the

overall performance of these algorithms. Specifically, given an integer n , a pair of circular-arc polygons with n edges are generated at random, and then each algorithm is executed alternately, using the pair of polygons as the input. This is done one thousand times. In each trial, the running time of each algorithm is recorded, and accumulated to previous trials. We compute the average value for estimating the average running time of each algorithm. Furthermore, we vary the value of n , and obtain the running time of each algorithm using the same method mentioned above.

8.3 Comparative results

The results of the first set of experiments are listed in Table 2 below. Specifically, the methods are listed in Row one, the average running time of each method is listed in Row two, and the improvement factors of our algorithm over the compared methods are shown in Row 3.

Method	Berberich	CGAL	Naive	Standard	RE2L
Time (sec.)	0.0287	0.0273	0.00239	0.00175	0.00112
Improvement	25.625	24.375	2.13	1.5625	—

TABLE 2

The average running time in the first set of experiments.

From this table, we can easily see that the proposed method outperforms other four methods, demonstrating the efficiency and effectiveness of our proposed method. Interestingly, the simpler versions of the proposed method yet outperforms the former two methods, let alone the proposed method. To some extent this verifies our previous claim — directly appealing to existing algorithms used to compute boolean operation of conic and/or general polygons is usually not efficient enough.

Compared to the former two methods, although the latter three ones adopt a different data structure, but we note that the fourth one also employs the plane sweep method, similar to the former two ones. Viewed from the theoretical perspective, the former two ones should not have such poor performance. To further verify this phenomenon and explain it, we hence conduct another set of experiments, evaluating the overall performance of these algorithms.

n	Berberich	CGAL	Naive	Standard	RE2L
5	0.0293	0.0281	0.00234	0.0018	0.00107
10	0.0772	0.0609	0.0062	0.0041	0.00256
20	0.1297	0.1282	0.0125	0.0072	0.00369
30	0.1741	0.1656	0.0328	0.0176	0.00614
40	0.5672	0.5172	0.0391	0.0182	0.00683
50	0.681	0.61	0.0594	0.0213	0.00851

TABLE 3

The average running time of each algorithm, where n denotes the number of edges of each polygon.

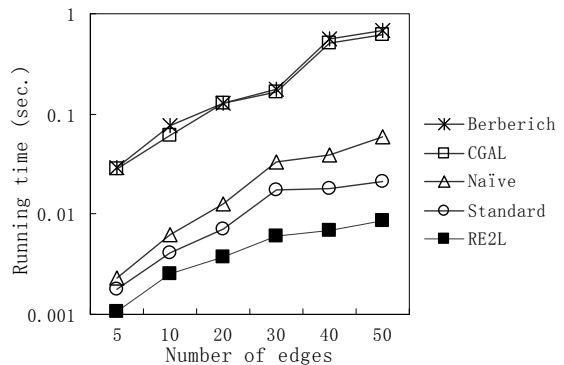


Fig. 7. The curve graph plotted using the data of Table 3.

Table 3 lists the detailed results of the second set of experiments. The corresponding curve graph is plotted in Figure 7 for the sake of intuition. As we expected, this set of results also show that the proposed method outperforms other four ones, and is several orders of magnitude faster than the former two ones. Compared to the fourth method, the better performance of our proposed method is ascribed to those optimization strategies, and the poorer performance of the third method is due to that computing the intersections in such a way is (somewhat) inefficiency. Particularly, this deficiency is more obvious when the number of edges of polygons is large (see Figure 7). By comparing the differences of these methods, we can easily see that the reason for the poorer performance of the former two methods may well be that both of methods employ the CGAL library and the DCEL structure¹. Furthermore, the set of results also show us that the proposed method has better scalability compared to other four ones, as the growth speed of the running time is slower than that of other four ones, when the number of edges of polygons increases.

9 EXTENSIONS

While this paper focuses on boolean operation of circular-arc polygons, our techniques can be easily extended to compute boolean operation of traditional polygons. Assume there are two traditional polygons for example, we can also use two double linked lists to represent them. In this case, the Tag domain is unneeded as the traditional polygons do not need the appendix points. We can also choose the *related edges* based on the extended boundary lines, and store them using *two sequence lists*. Note that the third domain of the sequence list is unneeded, as here

1. We remark that computing the intersections of two polygons is unavoidable for any clipping algorithm, and it is a dominant step [10], [7], [6]. Both the former two methods and the fourth one adopt the plane sweep method to compute the intersections, their performance differences however are so great. This reminds us that the gap may well be due to the usage of the CGAL library and the DCEL structure (the former might be the major reason). The further explanation is beyond the topic of this paper.

all related edges are straight line segments. When computing the intersections, we can also use *two labels* to speed up the process of inserting the intersections into their corresponding edges, and to avoid *false intersections*. Next, we also construct *two new linked lists*, by using the information stored in two sequence lists to replace the related edges in the original linked lists. Particularly, we here do not need to insert new appendix points and merge the decomposed arcs, as the traditional polygons have no such information. We finally get the resultant polygon by *traversing* the two new linked lists, it is the same as that in Section 6.

Furthermore, the discussions presented in previous sections assumed the circular-arc polygons to be operated have no holes. If we want to handle the opposite case, this can be easily achieved by a straightforward adaptation of our proposed method. Assume we want to compute the intersection of two circular-arc polygons with holes for example, we can use multiple double linked lists to represent the circular-arc polygon with holes. One is to represent the outer boundaries of the circular-arc polygon, others are respectively to represent the boundaries of each hole. We can first compute the intersection of the outer boundaries of two polygons, and then use this intersection result to subtract each hole of the two polygons. All of these steps are quite straightforward, when our proposed method is given beforehand.

10 CONCLUSION

This paper investigated the problem of boolean operation on circular-arc polygons. By well considering the nature of the problem, concise data structure and targeted algorithms were proposed. The proposed method runs in time $O(m + n + (l + k) * \log l)$, using $O(m + n + l)$ space. We conducted extensive experiments demonstrating the effectiveness and efficiency of the proposed method, and showed our techniques can be easily extended to compute boolean operation of other types of polygons.

REFERENCES

- [1] Cgal. <http://www.cgal.com>.
- [2] Lead. <http://www.lead.com>.
- [3] R. D. Andreev. Algorithm for clipping arbitrary polygons. *Computer Graphics Forum (CGF)*, 8(3):183–191, 1989.
- [4] J. L. Bentley and T. Ottmann. Algorithms for reporting and counting geometric intersections. *IEEE Transactions on Computers (TC)*, 28(9):643–647, 1979.
- [5] E. Berberich, A. Eigenwillig, M. Hemmer, S. Hert, K. Mehlhorn, and E. Schmer. A computational basis for conic arcs and boolean operations on conic polygons. In *European Symposium on Algorithm (ESA)*, pages 174–186. 2002.
- [6] M. de Berg, O. Cheong, M. van Kreveld, and M. Overmars. *Computational geometry: algorithms and applications, Third Edition*. Springer, Berlin, 2008.
- [7] J. D. Foley, A. van Dam, S. K. Feiner, and J. F. Hughes. *Computer Graphics: principles and practice, Second Edition*. Addison-Wesley, Massachusetts, 1996.
- [8] Y. Gardan and E. Perrin. An algorithm reducing 3d boolean operations to a 2d problem: concepts and results. *Computer-Aided Design (CAD)*, 28(4):277–287, 1996.
- [9] Y.-X. Gong, Y. Liu, L. Wu, and Y.-B. Xie. Boolean operations on conic polygons. *Journal of Computer Science and Technology (JCST)*, 24(3):568–577, 2009.
- [10] G. Greiner and K. Hormann. Efficient clipping of arbitrary polygons. *ACM Transactions on Graphics (TOG)*, 17(2):71–83, 1998.
- [11] J. E. Hopcroft and M. S. Karasick. Robust set operations on polyhedral solids. *IEEE Computer Graphics and Applications*, 9(6):50–59, 1989.
- [12] D. Krishnan and L. M. Patnaik. Systolic architecture for boolean operations on polygons and polyhedra. *Computer Graphics Forum (CGF)*, 6(3):203–210, 1987.
- [13] Y.-D. Liang and B. A. Barsky. An analysis and algorithm for polygon clipping. *Communications of the ACM (CACM)*, 26(11):868–877, 1983.
- [14] Y. K. Liu, X. Q. Wang, S. Z. Bao, M. Gombosi, and B. Zalik. An algorithm for polygon clipping, and for determining polygon intersections and unions. *Computers and Geosciences (GANDC)*, 33(5):589–598, 2007.
- [15] P.-G. Maillot. A new, fast method for 2d polygon clipping: Analysis and software implementation. *ACM Transactions on Graphics (TOG)*, 11(3):276–290, 1992.
- [16] A. Margalit and G. D. Knott. An algorithm for computing the union, intersection or difference of two polygons. *Computers and Graphics (CG)*, 13(2):167–183, 1989.
- [17] F. Martinez, A. J. Rueda, and F. R. Feito. A new algorithm for computing boolean operations on polygons. *Computers and Geosciences (GANDC)*, 35(6):1177–1185, 2009.
- [18] S. Meguerdichian, F. Koushanfar, M. Potkonjak, and M. B. Srivastava. Coverage problems in wireless ad-hoc sensor networks. In *IEEE International Conference on Computer Communications (INFOCOM)*, pages 1380–1387. 2001.
- [19] Y. Peng, J.-H. Yong, W.-M. Dong, and J.-G. S. Hui Zhang. A new algorithm for boolean operations on general polygons. *Computers and Graphics (CG)*, 29(1):57–70, 2005.
- [20] A. Rappoport. An efficient algorithm for line and polygon clipping. *The Visual Computer (VC)*, 7(1):19–28, 1991.
- [21] M. Rivero and F. R. Feito. Boolean operations on general planar polygons. *Computers and Graphics (CG)*, 24(6):881–896, 2000.
- [22] M. I. Shamos and D. Hoey. Geometric intersection problems. In *IEEE Symposium on Foundations of Computer Science (FOCS)*, pages 208–215. 1976.
- [23] I. E. Sutherland and G. W. Hodgman. Reentrant polygon clipping. *Communications of the ACM (CACM)*, 17(1):32–42, 1974.
- [24] B. R. Vatti. A generic solution to polygon clipping. *Communications of the ACM (CACM)*, 35(7):56–63, 1992.
- [25] B. Wang. Coverage problems in sensor networks: A surveys. *ACM Computing Surveys (CSUR)*, 43(4):1–53, 2011.
- [26] K. Weiler and P. Atherton. Hidden surface removal using polygon area sorting. In *International Conference on Computer Graphics and Interactive Techniques (SIGGRAPH)*, pages 214–222. 1977.